

Laboratory Testing to Address the Potential for Damaging Hydraulic Pressure in the Concrete Tie Rail Seat

TRB 11-3395

*Submitted for publication in the proceedings of the
Transportation Research Board 90th Annual Meeting*

15 November 2010

John C. Zeman^{1,3}, J. Riley Edwards², David A. Lange², and Christopher P. L. Barkan²

¹*Farnsworth Group, Inc. (Current Affiliation)
2709 McGraw Dr., Bloomington, IL 61704*

²*Railroad Engineering Program
Department of Civil and Environmental Engineering
University of Illinois at Urbana-Champaign
205 N. Mathews Ave., Urbana, IL 61801
Fax: (217) 333-1924*

Abstract (211 words) + Body (5,105 words) + 6 Figures + 2 Tables = 7,316 Total Words

John C. Zeman

(217) 377-7714

jzeman2@gmail.com

J. Riley Edwards

(217) 244-7417

jedward2@illinois.edu

David A. Lange

(217) 333-4816

dlange@illinois.edu

Christopher P.L. Barkan

(217) 244-6338

cbarkan@illinois.edu

³ Corresponding author

ABSTRACT

Rail seat deterioration (RSD) is the most critical problem with concrete tie performance on North American freight railroads. Currently, the problem is not sufficiently understood to enable development of effective solutions. RSD is considered to have up to six potential failure mechanisms: abrasion, freeze-thaw cracking, crushing, hydro-abrasive erosion, and hydraulic pressure cracking. This paper investigates hydraulic pressure cracking. To evaluate hydraulic pressure cracking, a laboratory test apparatus and procedure were devised to measure the surface water pressure in a laboratory rail seat using tie pads of differing material composition and geometry. Results show that the magnitude of the pressure generated and the rate of pressure dissipation with many load cycles depends on the pad material and surface geometry. Additionally, results from experimental testing show that pads or pad assemblies that do not seal water tend to reduce rail seat surface pressures. Comparing the effective stress model and the measured surface water pressures, hydraulic pressure cracking appears to be a feasible mechanism for RSD given the correct combination of high rail seat loads, sufficient moisture, and a tie pad surface that develops high pressure. Additionally, this paper provides an overview of the current North American railway industry understanding of the factors influencing the causes of RSD.

INTRODUCTION TO RAIL SEAT DETERIORATION (RSD)

Rail seat deterioration (RSD) is degradation underneath the rail on a concrete tie. This deterioration leads to track geometry defects such as wide gauge and allows for accelerated deterioration of the rail-to-tie fastening system. Conversely, it has also been noted that fastening system defects (e.g. loss of toe load or insulator material) can lead to RSD. RSD was first identified by North American railroads in the late 1980's (*T. Johns, unpublished 2009*). In the early-1990's, tests were conducted at the Transportation Technology Center's (TTC's) Facility for Accelerated Service Testing (FAST) to compare the resistance of different combinations of concrete ties and fastening system components to RSD (*1*). TTC's tests resulted in the identification of certain tie pads and pad assemblies that mitigated RSD to a manageable level, providing solutions which were sufficient for the North American freight loading conditions in the mid-1990's.

Since then, rail life has increased due to improved materials and maintenance practices and axle loads have increased. Consequently, the materials and designs that worked in the past to mitigate RSD are often inadequate today (*R. Reiff, unpublished 2009*). In response to the continued prevalence of RSD on primary freight corridors in North America, members of the American Railway Engineering and Maintenance-of-Way Association (AREMA) Committee 30 (Ties) recently formed a working group of railroad employees, suppliers, and researchers to address the problem. One of the first actions of this working group was to agree on the factors and causes of RSD (Tables 1 and 2).

TABLE 1 Relevance of the Causes of RSD to the Potential Concrete Deterioration Mechanisms.

Causes	Abrasion	Crushing	Freeze-Thaw	Hydraulic Pressure	Hydro-Abrasive
High stresses at rail seat	✓	✓		✓	✓
Relative motion at rail seat	✓	✓		✓	✓
Presence of moisture	✓	✓	✓	✓	✓
Presence of abrasive fines	✓				✓

TABLE 2 Summary of Internal and External Factors Related to the Causes of RSD.

	High Stresses at the Rail Seat	Relative Motion at the Rail Seat	Presence of Moisture	Presence of Abrasive Fines
Internal Factors	<p><i>Loss of proper rail cant</i></p> <ul style="list-style-type: none"> • Loss of material at rail seat • Loss of material at shoulder • Loss of toe load 	<p><i>Looseness of fastening system (loss of toe load)</i></p> <ul style="list-style-type: none"> • Loss of material at rail seat • Loss of material at shoulder • Yielded or fractured clips <p><i>Scrubbing action</i></p> <ul style="list-style-type: none"> • Poisson's ratio of tie pad 	<p><i>Tie pad seal</i></p> <ul style="list-style-type: none"> • Material properties and surface geometry of tie pad • Looseness of fastening system • Wear of rail seat and tie pad <p><i>Concrete saturation</i></p> <ul style="list-style-type: none"> • Permeability of concrete and rail seat surface 	<p><i>Tie pad seal</i></p> <ul style="list-style-type: none"> • Material properties and surface geometry of tie pad • Looseness of fastening system • Wear of rail seat and tie pad <p><i>Fines from wear of rail seat components</i></p>
External Factors	<p><i>High vertical loads</i></p> <ul style="list-style-type: none"> • Impact loads • Degraded track geometry <p><i>High L/V ratio</i></p> <ul style="list-style-type: none"> • Truck hunting • Over-/under-balanced speeds on curves • Sharp curves • Degraded track geometry <p><i>High longitudinal loads</i></p> <ul style="list-style-type: none"> • Steep grades • Thermal stresses in rail • Train braking and locomotive traction <p><i>Poor load distribution among adjacent ties</i></p> <ul style="list-style-type: none"> • Non-uniform track substructure • Non-uniform tie spacing • Degraded track geometry 	<p><i>Uplift action</i></p> <ul style="list-style-type: none"> • Low stiffness of track substructure, higher deflections <p><i>Lateral action</i></p> <ul style="list-style-type: none"> • Truck hunting • Truck steering around curves (push and pull) • Over-/under-balanced speeds on curves • Sharp curves <p><i>Longitudinal action</i></p> <ul style="list-style-type: none"> • Steep grades • Thermal stresses in the rail • Train braking and locomotive traction 	<p><i>Climate</i></p> <ul style="list-style-type: none"> • Average annual rainfall, days with precipitation, humidity, etc. • Average evaporation rate, etc. • Extreme daily or annual temperatures • Number of annual freeze/thaw cycles 	<p><i>Environment</i></p> <ul style="list-style-type: none"> • Wind-blown sand or dust • Moisture to transport the abrasive fines under the tie pad <p><i>Track maintenance</i></p> <ul style="list-style-type: none"> • Ground ballast • Metal shavings from rail grinding <p><i>Train operations</i></p> <ul style="list-style-type: none"> • Application of locomotive sand for braking (especially on grades) • Coal dust and other abrasive commodities

Table 2 separates the factors that contribute to the causes of RSD into both internal and external factors. Some factors are within the realm of concrete-tie design and others are functions of track alignment, track maintenance, train operations, or the climate/environment. Comparing Tables 1 and 2 highlights the fact that RSD is a complex interaction of different deterioration mechanisms and causes.

In addition to the challenge of diagnosing the mechanisms and causes of RSD, it is difficult to detect RSD without removing the rail and fastening system and examining the concrete rail seat. Maintenance measures currently used to combat RSD are regular replacement of the tie pad, periodic replacement of the fastening components, restoration of the proper rail seat surface with an epoxy or polyurethane, or removal of the whole tie from service (2, 3). A survey of freight railroads in the US and Canada conducted by the University of Illinois at Urbana-Champaign (UIUC) concluded that RSD was the most critical problem with concrete ties on their routes (4). Prestressed concrete ties have the potential to withstand a combination of heavy axle loads and high tonnage that other tie materials cannot. Also, ballasted concrete-tie track or slab track are the preferred method of track support for high-speed operations due to their stiff support and tighter geometric tolerances (2, 3). For these reasons, improving the performance of concrete ties will be very beneficial to the railroad industry.

In addition, learning how to effectively eliminate or mitigate RSD will reduce the risk of concrete ties failing prematurely or requiring excessive maintenance. This would lower the life-cycle costs and help make concrete ties a more viable economic alternative to timber ties in North America. The US and Canadian railroads have learned much about RSD since it was first identified in the mid-1980's (5), but the mechanics of the deterioration process are still not wholly understood.

Currently, there is evidence that abrasion, freeze-thaw cracking, crushing, hydro-abrasive erosion, and hydraulic pressure cracking may contribute to RSD (5, 6). Little evidence has been found to suggest that alkali-silica reactivity (ASR) is contributing to RSD and research and experimental testing at UIUC has ruled out cavitation erosion as a feasible RSD mechanism (4, 5, 7). This research study is an effort to understand the mechanics of the concrete deterioration in RSD by focusing on moisture-driven mechanisms, such as hydraulic pressure cracking. By understanding which deterioration mechanisms are acting on the concrete, it will be possible to develop more effective methods to solve or mitigate RSD.

The theory on hydraulic pressure cracking claims that pore pressures in the concrete become large enough that the concrete's tensile strength is exceeded, resulting in cracking or spalling (5). In order to evaluate the feasibility of this theory, two elements were examined: the specific pore pressure required to damage the concrete, and the expected pore pressure in a typical concrete railroad tie. Modeling was conducted to develop an effective stress model to examine the hydraulic pressure cracking mechanism (8). Additionally, previous research at UIUC investigated the sealing characteristics of tie pads (9). The tie-pad seal is important because its design directly influences the potential for intrusion of moisture and fines beneath the tie pad and the potential for hydraulic pressure cracking or hydro-abrasive erosion to damage the concrete at the rail seat (9).

The focus of this paper is the development, execution, and summarization of results from laboratory tests undertaken at UIUC to obtain greater insight into the potential moisture-related failure mechanisms associated with RSD.

LABORATORY TESTS

In previous work on hydraulic pressure cracking, it was assumed that the surface pressure p was equal to the uniform vertical load stress (5). A laboratory setup and procedure were devised to measure p in a saturated, laboratory rail seat for different tie pads and loading scenarios to determine the validity of this assumption and whether the tie pad material or surface geometry affects the pressure generated.

Materials

In order to measure surface water pressure developed by simulated rail car loads on a mock concrete tie rail seat, a 6,000-psig-rated (41.4-MPa-rated) pressure transducer was placed in a concrete block and protected by a steel pipe cast into the specimen. The concrete had an average 28-day compressive strength of approximately 8,000 psi (55.2 MPa), and the block was capped with a sulfur compound to improve the block and base plate interface. The pressure transducer's orifice has an inner diameter of 0.6 inches (15 millimeters) and is 3.75 inches (95 millimeters) deep, and was placed flush with the block's "rail seat" surface.

A 100-kip (445-kilonewton (kN)) MTS servo-hydraulic actuator was used to apply normal loads to the tie pads on top of the instrumented concrete blocks. The concrete blocks were placed in a steel-based, plexiglass tank to hold water during the tests (2, 3).

Nine tie pads of different materials and surface geometries were considered in this study, including three types of pad assemblies. The tie pad surfaces that were tested were flat polyurethane, grooved polyurethane, dimpled polyurethane, flat ethyl-vinyl acetate (EVA), dimpled EVA, dimpled santoprene, a studded pad with a flat plastic bottom (2-part C), a two-part assembly with a flat plastic bottom (2-part B), and a three-part assembly with a flat foam bottom underneath a steel plate (3-part A). Examples of the surface geometries are shown in Figure 1.

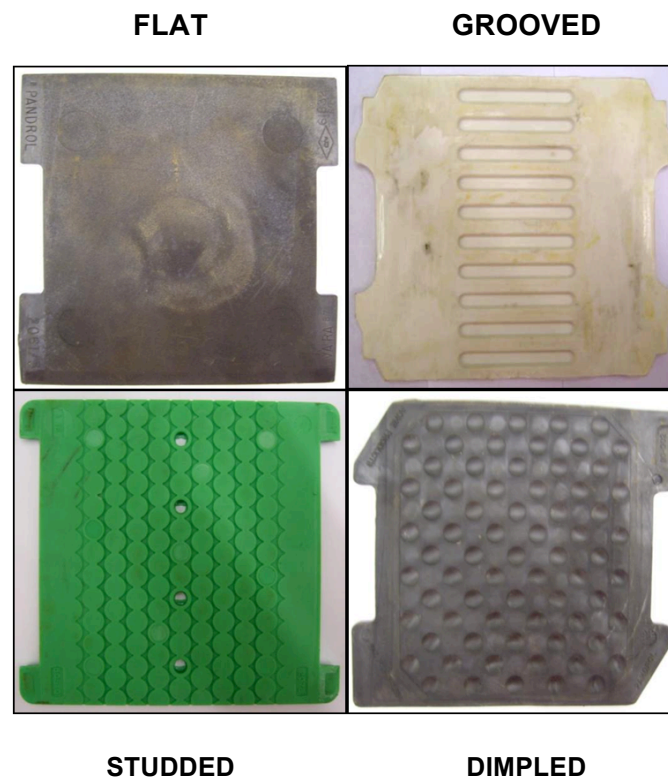


FIGURE 1 Tie pad surface geometries.**Procedure**

After applying some simplifying assumptions about a 286-kip (130-metric-ton) gross rail car load, the static normal force on one rail seat would be approximately 20 kips (89 kN), while an upper bound of dynamic normal force was approximated as 60 kips (3, 10).

Over 180 unique scenarios were tested for the load experiments, and at least one replication was conducted per scenario. The tests involved cyclic loading of the concrete block, cycling the load from a minimum of 5 kips (22 kN) up to a maximum load, chosen from 20, 30, 40, 50, or 60 kips (89, 134, 178, 223, or 267 kN). The waveform of the load was chosen from trapezoidal wave (ramping at 200 kips (890 kN) per second), square wave, or sinusoidal wave (frequency of 2 or 4 Hertz (Hz)). The trapezoidal and square wave tests were run at 0.5 Hz frequency. The water level in the tank was varied from 0 to 6 inches (15 centimeters) above the rail seat surface, with 6 inches (15 centimeters) being the typical water level.

When running the tests, water was filled to the desired level, the pad under consideration was placed on the block, and the actuator was lowered to a point of contact (arbitrarily defined as 200 lb of force) to secure the pad in place. When a pad with indentations was used, the dimensions of the pad and the block were used to align the pad indentations in a specific way relative to the transducer orifice. All tests were run for 30 seconds, so that a 4-Hz test contained 120 cycles, whereas a 0.5-Hz test contained 15 cycles. Between trials with no changes in the water level or pad, the pad was secured to the block while the actuator was raised to allow relaxation of the pad and return of any water that had been expelled from the rail seat during the previous trial. This seemed to be an effective method for creating repeatable results.

Results

The data were processed so that the peak pressure values were identified for each trial. The maximum surface pressure p was plotted versus the applied load P to illustrate the correlation between load and surface pressure. By plotting these p - P graphs, it became apparent that the pads exhibited three distinct behaviors related to how much pressure they developed with the same applied load. The first group was referred to as “flexible pads,” and these pads produced pressure close to, though slightly below, the uniform rail seat load stress that Bakharev had assumed (Figure 2). The second group of “semi-rigid pads” shown in Figure 3 produced trend lines significantly below, though parallel to, the ideal uniform rail seat stress. The third set of pads (the pad assemblies) are plotted in Figure 4. This set of pads generated little, if any, pressure relative to the other pads. See the Appendix for the conversions from US customary units to SI units.

The studded pad (the top layer of the 2-part C assembly), which was the only pad to have narrow channels running along its full length (providing openings at the pad boundaries), did not generate any significant pressure in any of its trials. The same results were observed when a dimpled pad and a grooved pad were modified to provide 2-millimeter-wide channels from the indentation above the transducer to the pads’ edges.

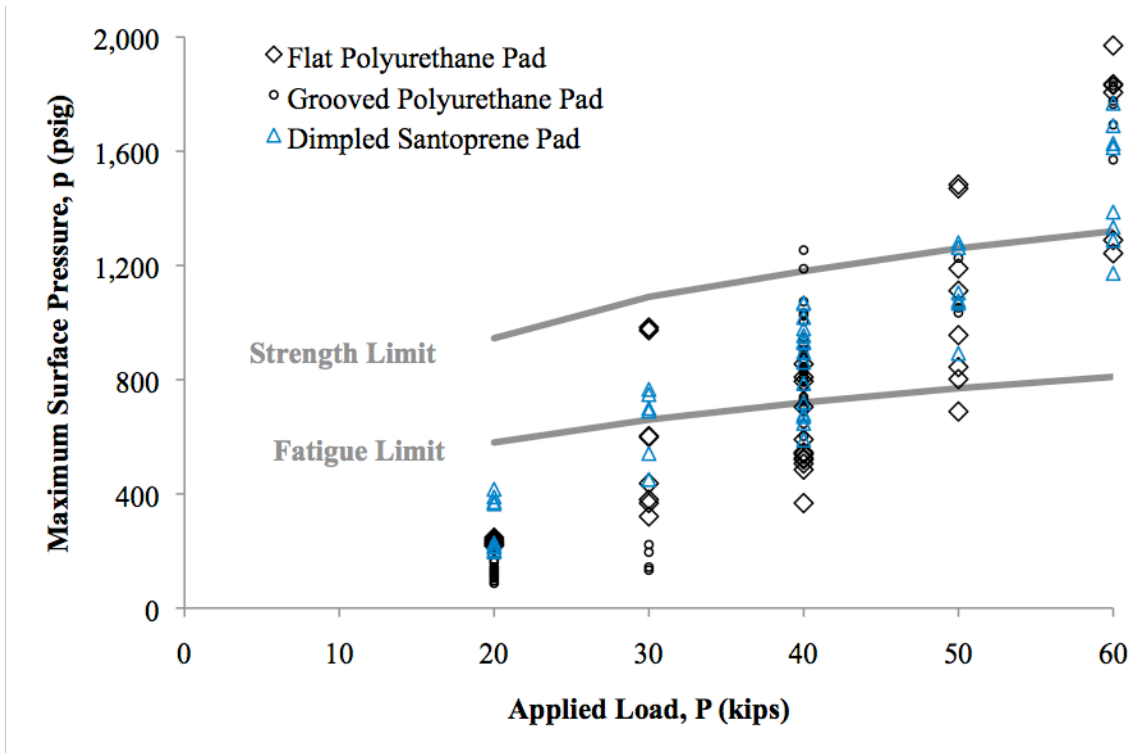


FIGURE 2 Comparing maximum surface pressure and damage limits, for flexible pads.

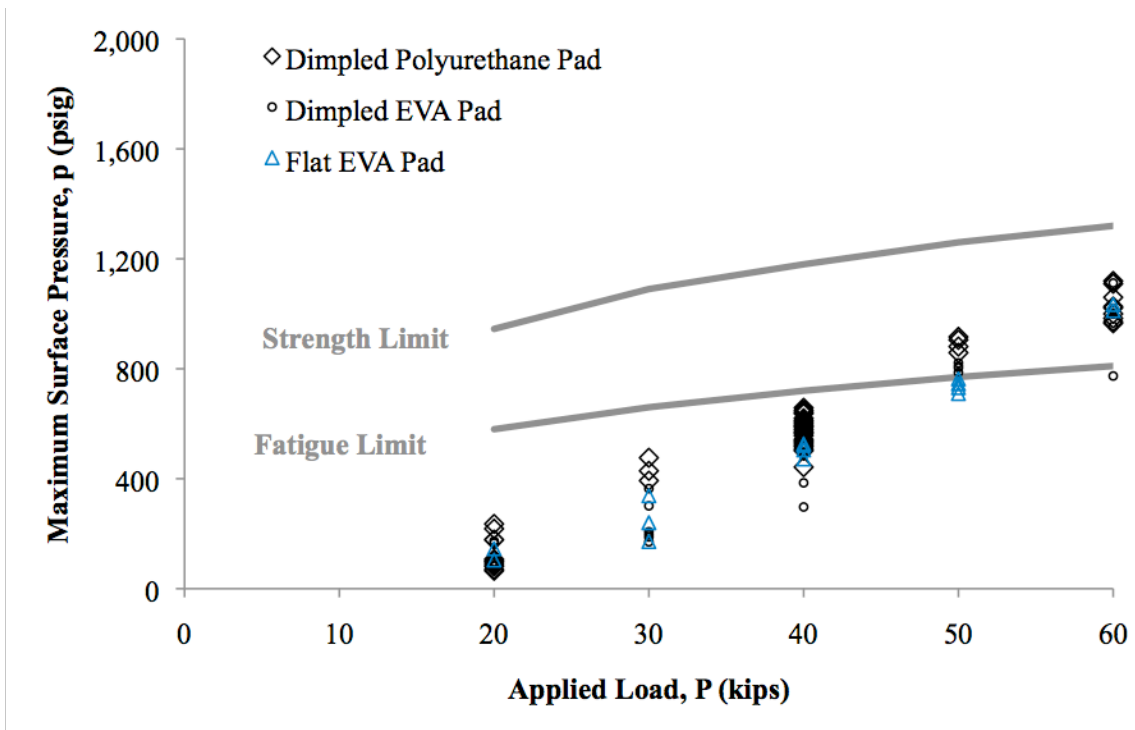


FIGURE 3 Comparing maximum surface pressure and damage limits, for semi-rigid pads.

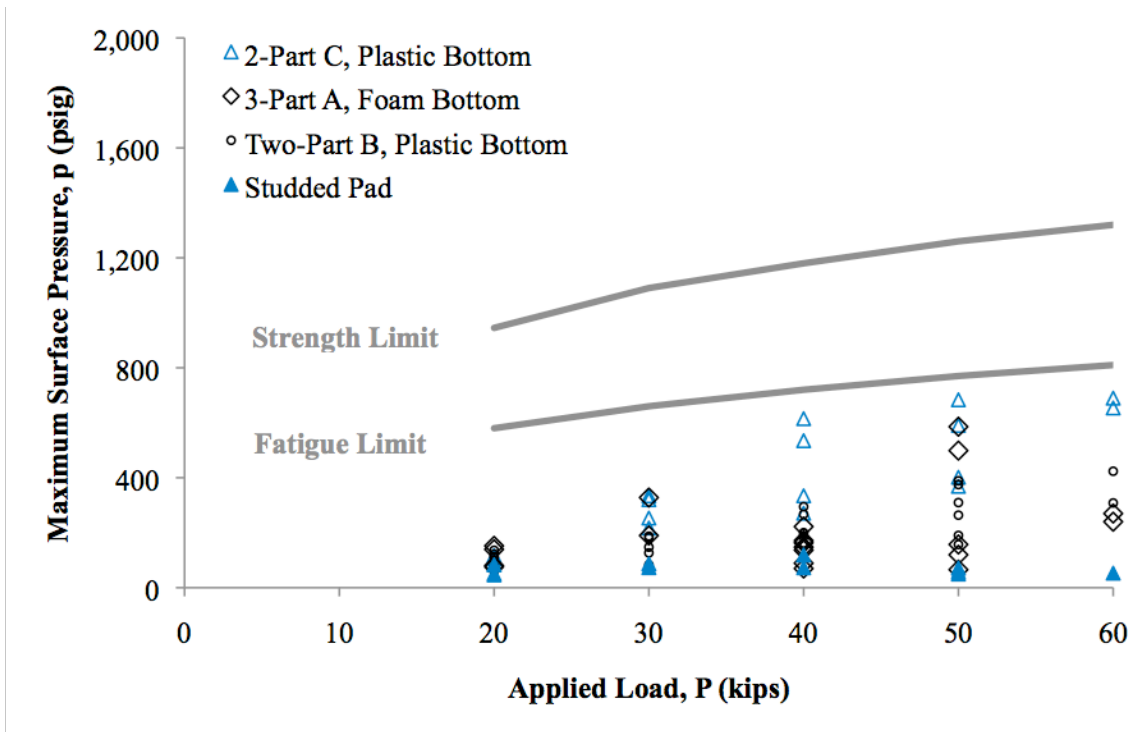


FIGURE 4 Comparing maximum surface pressure and damage limits, for pad assemblies with rigid layers.

The peak pressures p were plotted versus the load cycle count n to illustrate if and how the pressure varied during the course of a test. Some p - n data for a 40-kip (178-kN) applied load are presented here for the flexible pads in Figure 5 and for the semi-rigid pads in Figure 6. Typically, the maximum pressure occurred in the first few cycles of the trial. In some trials, the peak surface pressure was constant with continued load cycles. In other trials, the peak surface pressure dissipated from an initial maximum to either a steady state pressure that it sustained to the end of the trial, or a negligible value that was nominally zero pressure. The p - n data shown here for 40 kips (178 kN) are representative of the range of behavior that was observed for other magnitudes of applied load.

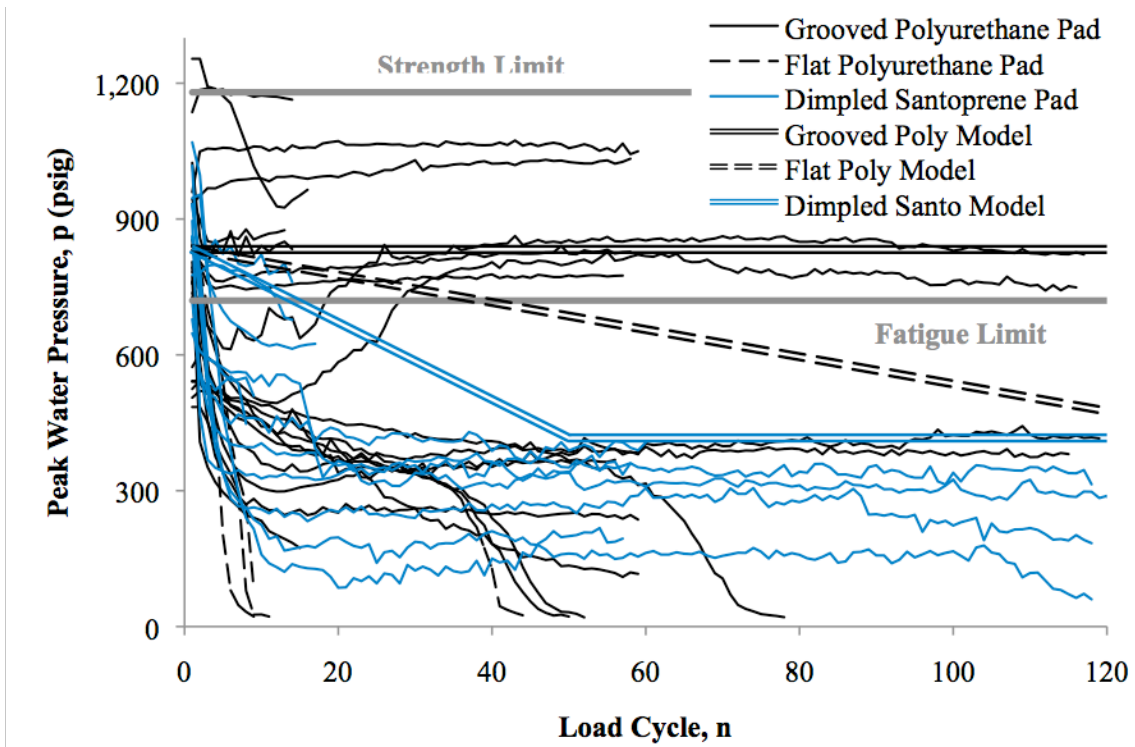


FIGURE 5 Recorded surface pressure peaks for flexible pads, 40-kip applied load.

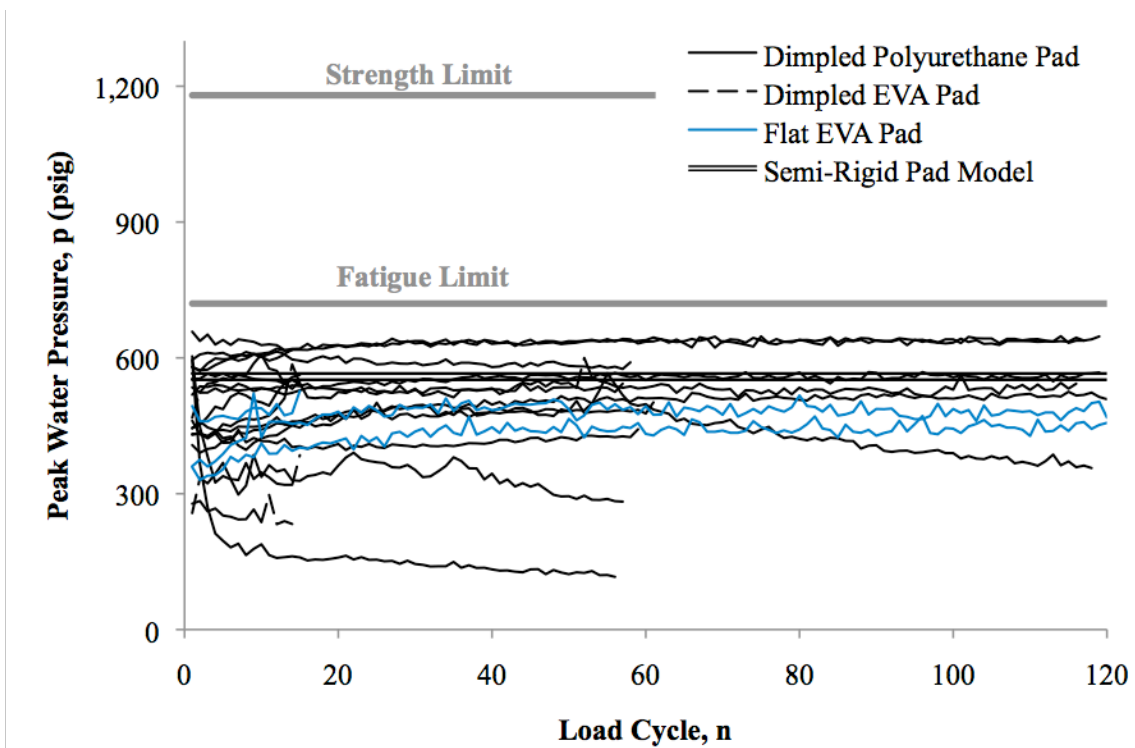


FIGURE 6 Recorded surface pressure peaks for semi-rigid pads, 40-kip applied load.

While running a series of tests, it was often observed that the actuator's loading plate would shift position relative to the block as a result of the flexibility of the frame. If the actuator-to-block interface was mismatched or if there was a nonzero contact angle it would have an effect on the p - n curves and the maximum pressure. As an example, the curves for flat polyurethane in Figure 5 came from two different test days, with the curves dropping to zero within 10 cycles occurring separately from the curves dropping to zero after 40 cycles. This difference may have been related to changes in the contact angle at the interface.

DISCUSSION

Sources of Variability

Linear trend lines fit the p - P data well for the thermoplastic pads, with the worst R-squared value at 0.72 for the flat polyurethane pad. The rest of the pads with trend lines had R-squared values at or above 0.88. There was significant scatter in the pad assembly data, yielding low R-squared values; however, because the pad assemblies also generated pressures below the predicted damage limits, the variability in their results was not a cause for concern. The p - P points plotted in Figures 2 through 4 include data from tests with different water levels, waveforms, and indentation alignments, where applicable. The fact that the data still plot with a good linear fit suggests that such parameters as surrounding water head and loading rate (train speed) do not have a strong influence on the surface pressure. Also, analysis isolating these two variables did not show any significant trends in the resulting surface pressure.

The most likely source of variability in the test results was the difficulty in controlling the contact angle between the loading plate and the rail seat block. Advancing the actuator with a nonzero contact angle between the loading plate and the block most likely provided the surface water a path for which it could escape more easily. Without a contact angle, there would be a greater chance that a seal would develop between the pad and the concrete before the surface water could be forced out (3). This may explain some of the scatter in the maximum pressure generated, as well as the variations in p - n behavior, particularly for the flat polyurethane's different pressure loss rates (Figure 5). The potential implications in track are that rail roll or tilt could lead to similar non-zero contact angles between the rail base and the rail seat. If a nonzero contact angle occurs, it may reduce the rail seat surface pressure that is generated in track.

It was difficult to control the contact angle because the test frame was too flexible for this application and a small change in the angle at the actuator's restrained pin connection would result in a significant change in the position of the loading plate. In other words, the unbraced length of the actuator was too long, and the test procedure required dimensional tolerances at the mock rail seat that were difficult to maintain with this test apparatus. A future test apparatus of this type should have a more rigid test frame, as long as adjustment can be made for misaligned surfaces (with a ball-and-socket joint, for example).

As for the variable p - n behavior of the grooved polyurethane pad (Figure 5), it appears that the trials with the greatest sustained pressure mostly occurred when the groove indentation (see Figure 1) was directly above the transducer. The set of trials with the pressure just above the fatigue limit mostly occurred when the transducer was aligned between two indentations, and the set of trials with the greatest pressure loss for the grooved polyurethane pad mostly came from the case of the transducer aligned with the long edge of an indentation. For the pads with indentations, some of the variability in p - n behavior may be explained by changes in indentation alignment.

Surface Water Pressure and Velocity

In Bakharev's model of hydraulic pressure, it was assumed that the surface pressure generated by a load P would be equal to P divided by the area of the rail seat, and this is referred to here as the uniform load stress. This assumes that the pad and the rail seat are separated by a film of water that transfers the load. For the surface water to ideally transfer load, a seal must be created between the tie pad and the concrete to prevent water from flowing rather than being pressurized. The p - P trend lines for the flexible pads are close to this ideal uniform load stress, suggesting that the flexible pads match Bakharev's assumption well.

The semi-rigid pads exhibited very consistent p - P behavior that was parallel to but significantly below the ideal rail seat load stress assumption. One way to explain these results is to consider the transfer of energy through the system. The applied load acts as an energy input that is transferred through the pad to the rail seat block. If water is between the pad and the rail seat, then energy is also transferred to the water. Borrowing from the Bernoulli equation for pipe flow, neglecting changes in elevation (II), we considered the surface water's total energy as the sum of its pressure energy and velocity energy. If a perfect seal is created, and there is no air in the transducer chamber, then all of the load energy would be transferred as pressure energy in the water. Neglecting any dynamic effects and assuming uniform load distribution, it can be assumed that the rail seat load stress is a maximum for the surface pressure that can be generated under a given load – representing the case where the total energy is pressure energy. If water is allowed to escape, fill air voids, or otherwise flow, then some of the energy would be manifested as velocity, reducing the pressure that can be generated. Allowing some of the water to escape or flow rather than become pressurized may explain the difference between the high- and low-pressure pads.

The concept of energy transfer can be applied to offer an explanation for the varied p - n results in Figures 5 and 6. There were three general types of p - n behavior observed: constant pressure with continued cycles, pressure loss from a maximum to a steady state value, and pressure loss from a maximum to zero. What may be causing pressure loss with load cycles is that some volume of water is forced out either from the transducer chamber or from the indentations of the pad. As a pad relaxes between cycles, there would still be at least 5 kips of load applied to the pad, so there may have been enough of a seal that water did not return between cycles. Rather, there might have been a reduced volume of water in the chamber or indentations, requiring the pad to locally flex more into the chamber to pressurize the water. As a result of this loss of contact with the water, the stress distribution over the pad may have changed such that most of the stress was transferred away from the transducer's orifice. If the volume of water in the transducer chamber became low enough, the pad may have been unable to contact the water and pressurize it, resulting in a reading of zero. Though this explanation of pressurization versus ejection was not specifically tested, it was found that the relative ranking of flexural stiffness of each pad aligned with the load-pressure groups, suggesting that flexural stiffness is a characteristic that relates to surface water pressurization.

Comparison of Tie Pads

The grooved and flat polyurethane pad surfaces were two sides of the same tie pad. These surfaces generated very similar p - P curves, but consistently different p - n behavior, providing strong evidence that indentations can lead to more sustained pressures with load cycles – the indentations may act as storage compartments for the surface water or they may introduce more tortuous escape paths than a flat surface would. However, the dimpled and flat EVA pads

generated similar p - P and p - n graphs, despite the difference in surface geometry. It is important to note that the dimpled EVA and flat EVA are different pads with different thicknesses, so it is not quite the same comparison as with the grooved and flat polyurethane. Generally EVA is a stiffer material than polyurethane. This introduces another complication when comparing these tie pads: though the two EVA pads are nominally the same material, there is room for variation of material properties to fit a specific product, similar to how a concrete mix is adjusted to produce different strengths. The same can be said about the dimpled and the flat polyurethane pads – they appear to have slightly different stiffness and hardness properties. The major difference between the dimpled santoprene and the dimpled polyurethane pads is that the santoprene rubber was relatively flexible and compressible and underwent permanent deformation after a few trials. The santoprene pad may have deformed enough that the dimples were flattened during the trials, causing it to act more like the flat polyurethane pad, in terms of surface pressure, than the dimpled polyurethane pad. It appears that both the surface geometry and the material properties of the pad determined what surface pressures were generated.

The studded pad, as well as the dimpled and grooved pads which were modified with channels, generated zero pressure for all tests, and this may have been because the surface water had at least one direct path to escape under applied load rather than being pressurized. As long as the escape velocity is less damaging than the pressure that would be generated, then providing escape channels in a thermoplastic material appears to be an effective way to prevent hydraulic pressure cracking in the rail seat.

It was observed that both the hardest material – the plastic bottom of the two-part assembly – and the softest material – the foam bottom of the three-part assembly – generated pressures lower than the semi-rigid pads. As shown in Figure 5, these pad assemblies developed pressures that would require very high rail seat loads – probably 80 to 90 kips (356 to 402 kN) or higher – to exceed the fatigue limit, assuming that the present data can be extrapolated. For the plastic bottoms, it is possible that it was difficult to create a seal with such a hard, stiff material, allowing water to flow rather than being pressurized. After one trial, the soft foam bottom would become permanently deformed. During the first trial, the foam apparently created an adequate seal and developed pressure not too far below the semi-rigid pads, with some pressure loss with load cycles. When a subsequent trial was run with the same pad, a lower pressure was obtained, and even lower pressures were generated with subsequently higher loads. This was observed when going from 50 kips to 60 kips (223 to 267 kN) in Figure 5 (from 30 kips to 40 kips (134 to 178 kN) as well). It may be that the deformation of the foam prevented the formation of a seal and allowed the water to escape. Another possible explanation is that the pressure behavior of the three-part assembly was dominated by the stiff metal layer in the middle, which would not readily form a seal. Also, it may be some combination of the deformation of the foam surface and rigidity of the metal layer.

CONCLUSION

Based on the results of the laboratory experiments and the damage limits defined by the effective stress model, hydraulic pressure cracking appears to have the potential to initiate or contribute to RSD as a concrete deterioration mechanism. It appears that the most effective way to prevent hydraulic pressure is to use pads or pad assembly bottoms that do not seal water. The soft foam with a rigid metal layer and the hard plastic bottoms developed little surface pressure at the rail seat, with the hard plastic being slightly more effective. When thermoplastic pads are in contact with the concrete rail seat, it appears that designing the pad with direct escape channels for the

water effectively ejects the surface water upon load application rather than pressurizing it. Thermoplastic pads without escape channels created the highest surface pressures, apparently sealing the water during load application. It seems advisable and relatively simple to incorporate these considerations into future pad and pad assembly designs; however, these design considerations for hydraulic pressure must be balanced with the possibility that allowing water and fines to flow in and out might increase wear due to hydro-abrasive erosion and abrasion. The potential for hydro-abrasive erosion to damage concrete seems feasible, but more research is needed to understand how important this mechanism is before design recommendations can be made.

Low rail seat loads, resulting from near-static wheel loads and good load distribution among adjacent ties, will not generate damaging hydraulic pressure at the rail seat, according to the effective stress model. In some cases, sufficient moisture for critical saturation is required for hydraulic pressure to damage the concrete. Furthermore, the concrete strength should play a major role in determining whether the hydraulic pressures are damaging. What remains is the possibility that hydraulic pressure could initiate microcracking by exceeding the concrete strength. However, according to the results of this investigation, the same preventative measures listed above could cause the likelihood of this scenario to be insignificant as well.

ACKNOWLEDGMENTS

This project is sponsored by a grant from the Association of American Railroads (AAR) Technology Scanning Program. The authors would like to thank David Davis and Richard Reiff of TTCI; Ernie Barenberg, Grzegorz Banas, and Tim Prunkard of the University of Illinois at Urbana-Champaign (UIUC); Bill Riehl of RailAmerica Inc.; Dwain Jackson of Transducers Direct; the AAR Technology Scanning Committee; and the members of AREMA Committee 30 – Ties, Subcommittee 4 – Concrete Tie Technology for their invaluable contributions to this research. The authors would also like to acknowledge Mauricio Gutierrez-Romero, Mark Dinger, Kevin Kilroy, Hammad Khalil, Charles Gross, Samantha Chadwick, David Marks, and Joseph Rudd from UIUC and Edgardo Santana-Santiago of the University of Puerto Rico at Mayaguez for their work on this project. John C. Zeman has been supported in part by a CN Research Fellowship in Railroad Engineering. J. Riley Edwards has been supported in part by grants to the UIUC Railroad Engineering Program from CN, CSX, Hanson Professional Services, Norfolk Southern, and the George Krambles Transportation Scholarship Fund.

REFERENCES

- (1) Reiff, R., 1995, "An Evaluation of Remediation Technologies for Concrete Tie Rail Seat Abrasion in the FAST Environment," American Railway Engineering Association Bulletin, v 96, bulletin 753, Washington, DC, pp. 406-418.
- (2) Zeman, J.C., J.R. Edwards, D.A. Lange, C.P.L. Barkan, "Investigating the Role of Moisture in Concrete Tie Rail Seat Deterioration," AREMA Conference Proceedings 2009, American Railway Engineering and Maintenance-of-way Association (AREMA), Landover, Maryland, September 2009.
- (3) Zeman, J.C., J.R. Edwards, D.A. Lange, C.P.L. Barkan, "Investigation of Potential Concrete Tie Rail Seat Deterioration Mechanisms: Cavitation Erosion and Hydraulic Pressure Cracking," Proceedings of the Transportation Research Board 89th Annual Meeting, Washington, DC, January 2010.

- (4) Zeman, J.C., J.R. Edwards, D.A. Lange, C.P.L. Barkan, "Failure Mode and Effect Analysis of Concrete Ties in North America," Proc. of the 9th International Heavy Haul Conference, Shanghai, China, June 2009.
- (5) Bakharev, T., Chapters 1, 2, 3, 5, 6, and 7, Microstructural Features of Railseat Deterioration in Concrete Railroad Ties, M.S. Thesis, University of Illinois at Urbana-Champaign, Urbana, Illinois, 1994, pp. 1-28 and 68-97.
- (6) Choros, J., B. Marquis, M. Coltman, "Prevention of Derailments due to Concrete Tie Rail Seat Deterioration," Proceedings of the ASME/IEEE Joint Rail Conference and the ASME Internal Combustion Engine Division, Spring Technical Conference 2007, pp. 173-181.
- (7) Zeman, J.C., Hydraulic Mechanisms of Concrete-Tie Rail Seat Deterioration, M.S. Thesis, University of Illinois at Urbana-Champaign, Urbana, Illinois. 2010.
- (8) Zeman, J.C., J.R. Edwards, C.P.L. Barkan, D.A. Lange, 2010b, "Evaluating the Potential for Damaging Hydraulic Pressure in the Concrete Tie Rail Seat," Proceedings of the 2010 Joint Rail Conference, Urbana, Illinois, April 2010.
- (9) Zeman, J.C., J.R. Edwards, D.A. Lange, C.P.L. Barkan, "Sealing Characteristics of Tie Pads on Concrete Crossties," AREMA Conference Proceedings 2010, American Railway Engineering and Maintenance-of-way Association (AREMA), Landover, Maryland, August 2010.
- (10) *AREMA Manual for Railway Engineering*, American Railway Engineering and Maintenance-of-Way Association (AREMA), Landover, Maryland, 2009, v 1, ch. 30, parts 2 and 4.
- (11) Munson, B.R., D.F. Young, T.H. Okiishi, *Fundamentals of Fluid Mechanics*, 5th ed., John Wiley & Sons, Inc., Hoboken, New Jersey, 2006, ch. 2, 8, and 9 and Appendix B, pp. 39, 402-407, 489-492, 761.

APPENDIX**Conversions From US Customary Units to SI Units.**

Depth		Pressure		Load	
<i>in</i>	<i>cm</i>	<i>psi</i>	<i>MPa</i>	<i>kips</i>	<i>kN</i>
1	2.5	300	2.1	10	45
2	5.1	400	2.8	20	89
3	7.6	500	3.4	30	134
4	10.2	600	4.1	40	178
5	12.7	800	5.5	50	223
		900	6.2	60	267
		1000	6.9		
		1200	8.3		
		1500	10.3		
		1600	11.0		
		2000	13.8		